NF-κB regulates GDF-15 to suppress macrophage surveillance during early tumor development

Nivedita M. Ratnam, … , David J. Wang, Denis C. Guttridge

Research Article Cell biology Immunology

Macrophages are attracted to developing tumors and can participate in immune surveillance to eliminate neoplastic cells. In response, neoplastic cells utilize NF-κB to suppress this killing activity, but the mechanisms underlying their self-protection remain unclear. Here, we report that this dynamic interaction between tumor cells and macrophages is integrally linked by a soluble factor identified as growth and differentiation factor 15 (GDF-15). In vitro, tumor-derived GDF-15 signals in macrophages to suppress their proapoptotic activity by inhibiting TNF and nitric oxide (NO) production.

In vivo, depletion of GDF-15 in *Ras*-driven tumor xenografts and in an orthotopic model of pancreatic cancer delayed tumor development. This delay correlated with increased infiltrating antitumor macrophages. Further, production of GDF-15 is directly regulated by NF-κB, and the colocalization of activated NF-κB and GDF-15 in epithelial ducts of human pancreatic adenocarcinoma supports the importance of this observation. Mechanistically, we found that GDF-15 suppresses macrophage activity by inhibiting TGF-β–activated kinase (TAK1) signaling to NF-κB, thereby blocking synthesis of TNF and NO. Based on these results, we propose that the NF-κB/GDF-15 regulatory axis is important for tumor cells in evading macrophage immune surveillance during the early stages of tumorigenesis.

Find the latest version:

https://jci.me/91561/pdf

NF-κB regulates GDF-15 to suppress macrophage surveillance during early tumor development

Nivedita M. Ratnam,[1,2,3] Jennifer M. Peterson,[1,3] Erin E. Talbert,[1,3] Katherine J. Ladner,[1,3] Priyani V. Rajasekera,[1,3] Carl R. Schmidt,[4] Mary E. Dillhoff,[4] Benjamin J. Swanson,[5] Ericka Haverick,[4] Raleigh D. Kladney,[1,3] Terence M. Williams,[6] Gustavo W. Leone,[1,2,3] David J. Wang,[1,3] and Denis C. Guttridge[1,2,3]

[1]Department of Cancer Biology and Genetics, [2]Molecular, Cellular and Developmental Biology Graduate Program, [3]Arthur G. James Comprehensive Cancer Center, [4]Division of Surgical Oncology, [5]Department of Pathology, and [6]Department of Radiation Oncology, The Ohio State University (OSU), Columbus, Ohio, USA.

Macrophages are attracted to developing tumors and can participate in immune surveillance to eliminate neoplastic cells. In response, neoplastic cells utilize NF-κB to suppress this killing activity, but the mechanisms underlying their self-protection remain unclear. Here, we report that this dynamic interaction between tumor cells and macrophages is integrally linked by a soluble factor identified as growth and differentiation factor 15 (GDF-15). In vitro, tumor-derived GDF-15 signals in macrophages to suppress their proapoptotic activity by inhibiting TNF and nitric oxide (NO) production. In vivo, depletion of GDF-15 in *Ras*-driven tumor xenografts and in an orthotopic model of pancreatic cancer delayed tumor development. This delay correlated with increased infiltrating antitumor macrophages. Further, production of GDF-15 is directly regulated by NF-κB, and the colocalization of activated NF-κB and GDF-15 in epithelial ducts of human pancreatic adenocarcinoma supports the importance of this observation. Mechanistically, we found that GDF-15 suppresses macrophage activity by inhibiting TGF-β–activated kinase (TAK1) signaling to NF-κB, thereby blocking synthesis of TNF and NO. Based on these results, we propose that the NF-κB/GDF-15 regulatory axis is important for tumor cells in evading macrophage immune surveillance during the early stages of tumorigenesis.

Introduction

Transformation of normal cells to a neoplastic state requires multiple genetic changes, resulting in the activation of oncogenes and inhibition of tumor-suppressor genes (1). In this process, transformed cells attract innate and adaptive immune cells (1). Immune cells that infiltrate into the site of an initiating tumor exhibit antitumor activities as part of an "immune surveillance" function (2). Overcoming immune surveillance is essential for tumor development and is considered a critical hallmark of cancer (3). Indeed, current cancer immunotherapies take advantage of this feature by pharmacologically enabling key events that mediate antitumor surveillance (4).

Macrophages are the predominant population of immune cells that infiltrate an early developing tumor. These infiltrating macrophages are subsequently activated by a host of factors, such as damage-associated pattern molecules and tumor cell DNA (5, 6). Upon activation, macrophages function to directly eliminate tumor-initiating cells by secreting cytotoxic factors such as TNF and nitric oxide (NO) or by relaying tumor antigens to activate cytotoxic T cells (4, 5).

NF-κB is a transcription factor known to participate in the communication between tumor and immune cells (7). The NF-κB subunit p65 (also named RelA) is ubiquitously expressed in mammalian cells and, when constitutively activated, is associated

with cellular transformation (8). Studies indicate that constitutive NF-κB activity contributes to cancer cell proliferation, survival, and metastasis (9). Although established as an oncogene during the late stages of cancer progression, comparatively little is known about the effects of this pathway at the earlier stages of tumor development. Recent work from our laboratory showed that NF-κB functions as an oncogene by protecting *Ras*-expressing transformed cells from the actions of infiltrating innate immune cells (10). However, the mechanism by which NF-κB evades the antitumor effects of macrophages has not been established. Here, we identify growth and differentiation factor 15 (*Gdf-15*), also known as macrophage inhibitory cytokine 1 (*Mic-1*), as an NF-κB–regulated gene whose production by tumor cells and signaling in macrophages serves as an important promoter of early cancer development.

Results

GDF-15 protects transformed cells against macrophage-mediated killing. We recently discovered that transformed cells containing NF-κB are capable of circumventing the antitumor activity of activated macrophages (10). To determine whether this protective activity was mediated through a soluble factor, we utilized a coculture system containing peritoneal macrophages along with *p65+/+* or *p65−/−* immortalized mouse embryonic fibroblasts (MEFs) transformed with oncogenic *HRas* (*Ras* MEFs). Previous results had shown that, compared with *p65+/+Ras* cells, *p65−/−Ras* MEFs were more sensitive to the killing activity of macrophages (10). However, the killing of *p65−/−Ras* MEFs by macrophages was completely blocked when conditioned medium from *p65+/+Ras* MEFs
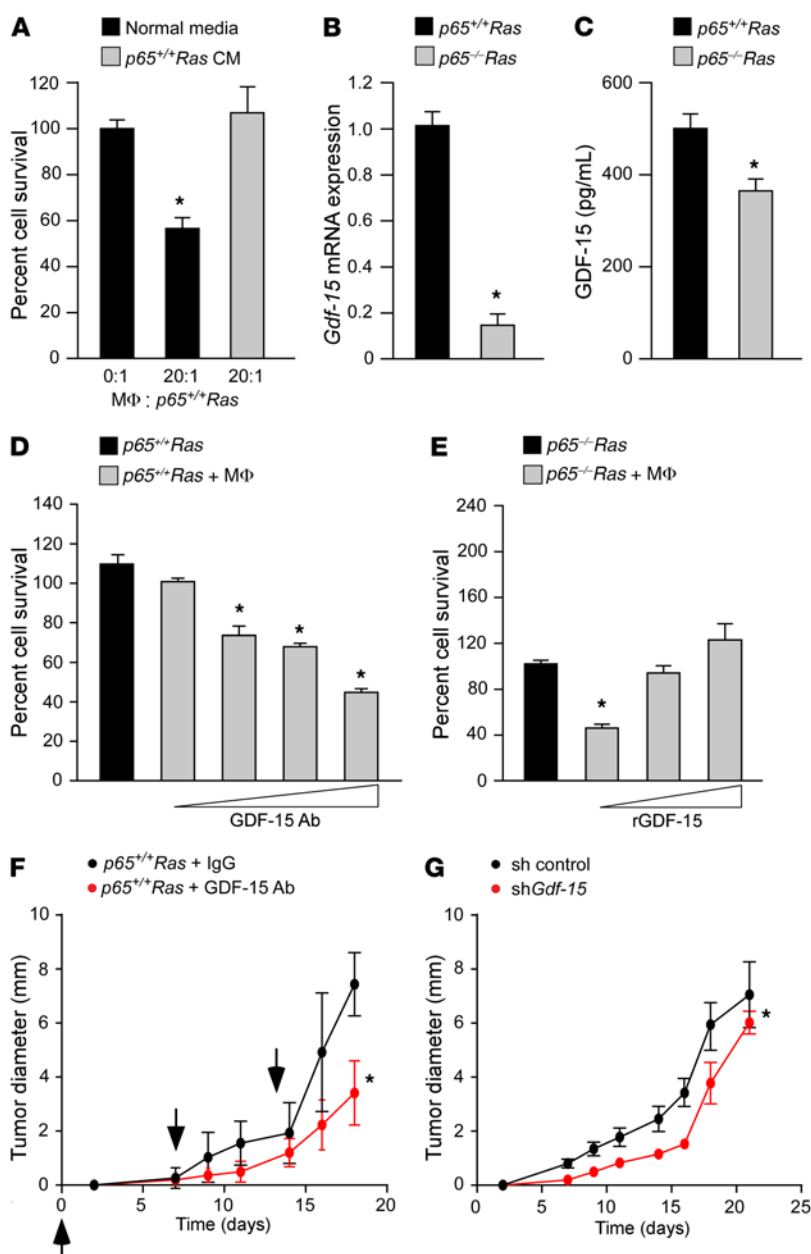
Figure 1. GDF-15 protects transformed cells against macrophages and promotes tumor development in vivo. (A) *p65⁻/⁻Ras* MEFs were cocultured with peritoneal macrophages (MΦ) with normal or conditioned media from *p65⁺/⁺Ras* MEFs. Graph represents cell survival scored by trypan blue exclusion, normalized to untreated *p65⁻/⁻Ras* MEFs. *n* = 6. Data are shown as mean ± SEM. *P ≤ 0.05, 1-way ANOVA. **(B)** *Gdf-15* analyzed by qRT-PCR in *Ras* MEFs normalized to *Gapdh* ± SEM. *P ≤ 0.05, Student's *t* test. *n* = 3. **(C)** GDF-15 ELISA from *Ras* MEF–conditioned media. *n* = 3. Data are shown as mean ± SEM. *P ≤ 0.05, Student's *t* test. **(D)** *Ras* MEFs were cocultured with macrophages and GDF-15–neutralizing antibody (GDF-15 Ab) at concentrations of 0, 25, 625, and 2,500 ng/ml. Graph represents cell survival similar to that shown in **A**. Data are shown as mean ± SEM from 2 independent experiments, each performed in triplicate. *P ≤ 0.05, 1-way ANOVA. **(E)** *p65⁻/⁻Ras* MEFs were cocultured with macrophages and recombinant GDF-15 (rGDF-15) at concentrations of 0, 5, and 10 ng/ml. Graph represents cell survival similar to that shown in **A**. Data represent mean ± SEM derived from 2 independent experiments, each performed in triplicate. *P ≤ 0.05, 1-way ANOVA. **(F)** *p65⁺/⁺Ras* MEFs (1 × 10⁶) were injected subcutaneously into SCID mice. Cohorts of mice (*n* = 5) were intravenously injected with GDF-15 antibody (20 μg/mouse) or IgG control (20 μg/mouse) and tumor sizes measured. Arrowheads indicate time points for injections. Data are shown as mean ± SEM. *P ≤ 0.05, SPSS repeated measures, general linear model. **(G)** Single clones from *Ras* MEFs expressing *Gdf-15* shRNA or scrambled control (sh control) were subcutaneously injected into SCID mice and tumor sizes measured. Data represent mean tumor diameter from 2 single clones (Scr-1 and Scr-2 for scrambled controls and C2 and D2 for *Gdf-15*–knockdown) injected into 5 mice each. Data are shown as mean ± SEM. *P ≤ 0.05, SPSS repeated measures, general linear model.

was added to the culture (Figure 1A). Similar results were obtained when cocultures were performed with bone marrow macrophages, indicating that the cytotoxic effect was not limited to a specific source of activated macrophages (Supplemental Figure 1, A–C; supplemental material available online with this article; https://doi.org/10.1172/JCI91561DS1). Together, these findings suggest that an NF-κB–dependent secreted factor protects transformed cells against the cytotoxic activity of inflammatory macrophages.

To identify the secreted factor, we performed RNA sequencing on *p65⁺/⁺* and *p65⁻/⁻* MEFs. We found that 1,946 genes were downregulated in *p65⁻/⁻* MEFs in comparison with *p65⁺/⁺* cells. Gene ontology (GO) analysis revealed that 138 of these differentially regulated genes coded for secreted proteins. These genes were then grouped based on their biological function. From this grouping, 51 were classified under response to endogenous stimuli, a category defined by the function of a gene that participates

in cellular movement, secretion, enzyme production, and gene expression (Supplemental Figure 1D). Within this gene set, one gene in particular, *Gdf-15*, drew our attention, since this cytokine is elevated in numerous cancers and has been shown to alter the activation of macrophages in response to lipopolysaccharide (11). GDF-15 is a member of the TGF-β superfamily of cytokines, yet how this cytokine regulates macrophage activation and whether such regulation is relevant in oncogenesis has not been explored.

To initiate our investigation of GDF-15, we first validated the findings from our RNA sequencing (RNA-seq) data set. Real-time quantitative real time PCR (qRT-PCR) results showed that *Gdf-15* was higher in *p65⁺/⁺* compared with *p65⁻/⁻* MEFs (Supplemental Figure 1E). Similar results were obtained from Ras-expressing *p65⁺/⁺* and *p65⁻/⁻* MEFs (Figure 1B), demonstrating that *Gdf-15* regulation is maintained in *Ras*-transformed cells. ELISAs performed with conditioned media also showed that the level of secreted GDF-15
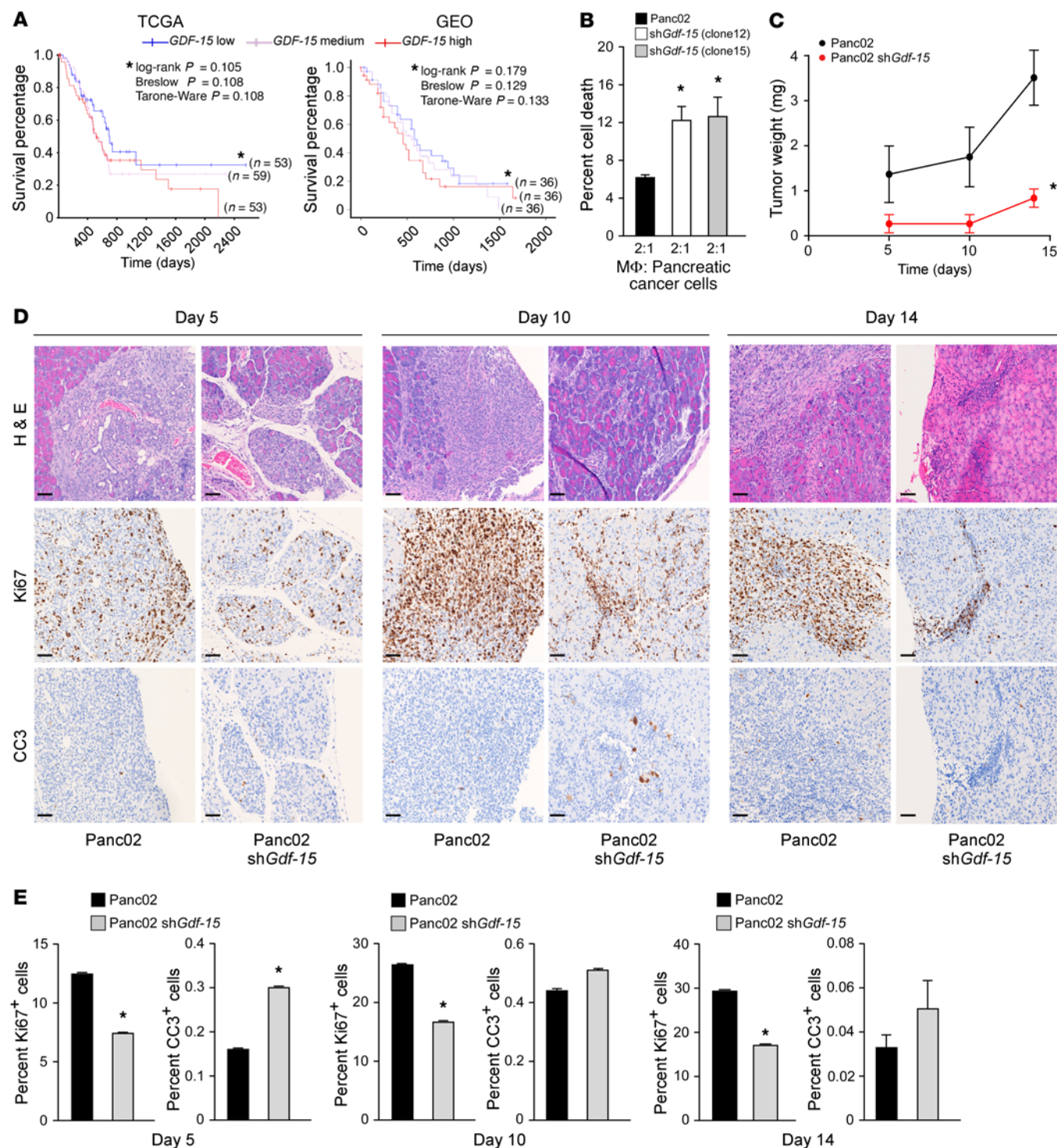
Figure 2. GDF-15 is required for early development of Panc02 tumors. (**A**) Kaplan-Meier curve assessing the effects of *GDF-15* expression on patient survival obtained from 165 patients in TCGA and 108 patients from a published study on the GEO database (ref. 13). Blue line represents PDAC patients with low *GDF-15* expression, white line represents patients with medium *GDF-15*, and red line indicates patients with high *GDF-15*. Asterisks compare *GDF-15* high and low groups. (**B**) Panc02 cells expressing an shRNA against *Gdf-15* (2 clones, numbers 12 and 15) were cocultured with peritoneal macrophages for 48 hours. The cells were then stained for annexin V, 7-AAD, and CD11b and analyzed by flow cytometry. CD11b⁻ cells positive for annexin V, 7-AAD, or both were graphed as percentage of cell death. Data represent mean ± SEM from 2 individual experiments, performed in triplicate. *$P \le 0.05$, 1-way ANOVA. (**C**) Panc02 control and Panc02 *Gdf-15*–knockdown cells (described above as clone 12) were injected orthotopically into the tail of the pancreas in C57BL/6 mice. Tumor weight was measured as weight of pancreas with tumor minus average weight of Matrigel-injected pancreas. Data represent the average tumor weight from cohorts of 5 to 7 mice per group per time point ± SEM. *$P \le 0.05$, SPSS repeated measures, general linear model. (**D**) Control and *Gdf-15*–knockdown orthotopic tumors described in **C** were sectioned and analyzed for H&E, Ki67, and CC3. Original magnification, ×20. Scale bars: 15 μm. (**E**) Ki67 and CC3 staining was quantitated and graphed from 5 mice per condition at each time point, from 5 random fields of view of the tumor area per mouse. Mean ± SEM. *$P \le 0.05$, Student's *t* test.
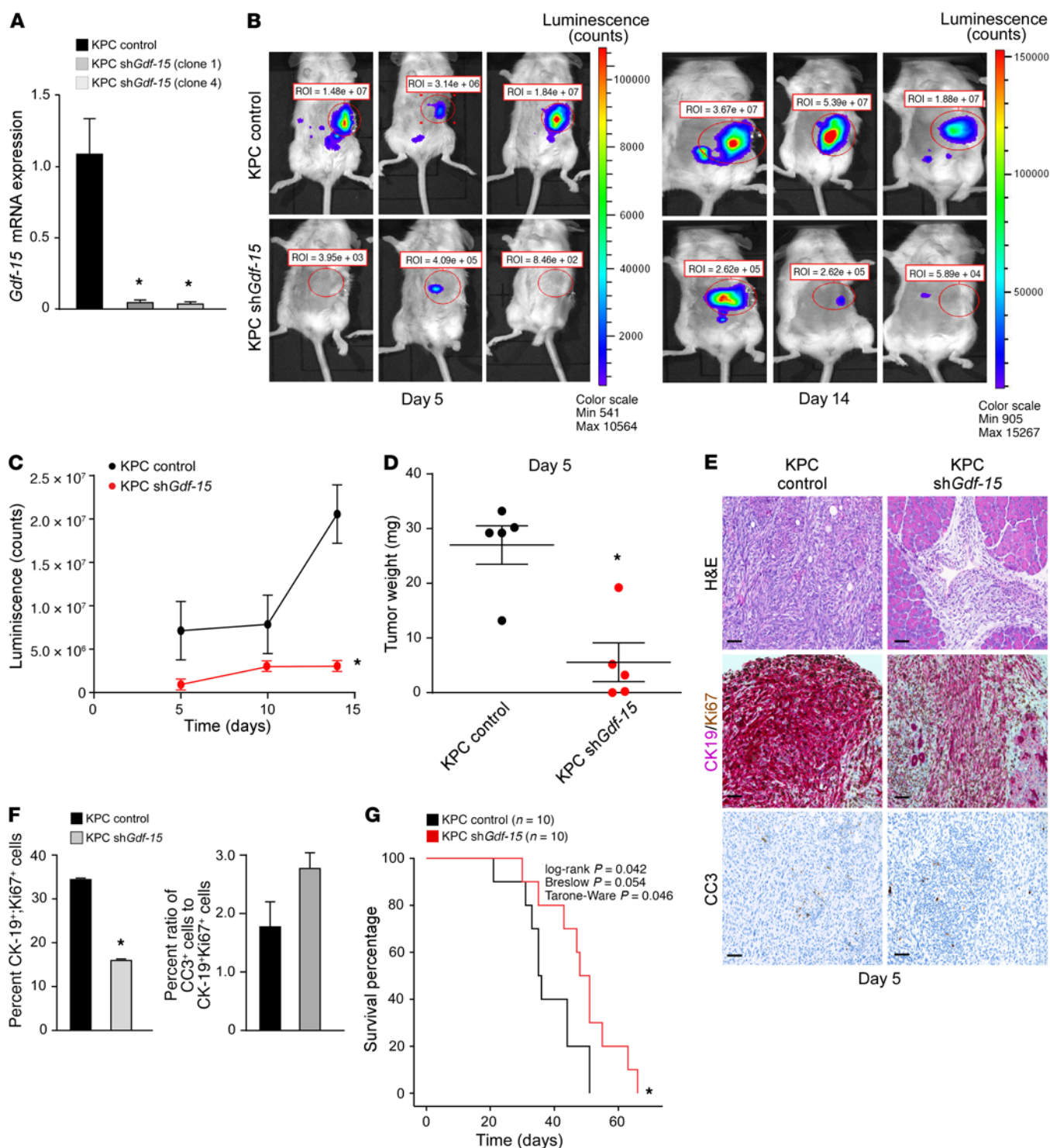
Figure 3. GDF-15 is required for development of KRas-induced PDAC. (**A**) KPC cells expressing an shRNA against *Gdf-15* were generated (2 clones, 1 and 4). Data are plotted as average gene expression (normalized to *Gapdh*) ± SEM. *n* = 3. *$P \leq 0.05$, Student's *t* test. (**B**) KPC control and KPC *Gdf-15*–knockdown cells (described above as clone 1) were injected orthotopically into the tail of the pancreas in C57BL/6 albino mice. Tumor growth was tracked by biolumi-nescence imaging. Shown are representative images tracking tumor growth of the mice. (**C**) The graph represents tumor growth derived from biolumines-cence measured in **B**. *n* = 6 per cohort. Data are shown as mean ± SEM. *$P \leq 0.05$, SPSS repeated measures, general linear model. (**D**) KPC control and KPC *Gdf-15*–knockdown cells (described above as clone 1) were injected orthotopically into the tail of the pancreas in C57BL/6 albino mice. The graph represents the average weight of tumors obtained from cohorts of 5 mice per condition similar to what is shown in Figure 2C. *$P \leq 0.05$, Student's *t* test. (**E**) Control and *Gdf-15*–knockdown orthotopic tumors were analyzed for H&E, CK19, and Ki67 colocalization and CC3. Original magnification, ×20. Scale bar: 15 μm. (**F**) CK19 (cytoplasmic, pink)/ Ki67 (nuclear, brown) dual staining was quantitated and graphed from 5 mice per condition from at least 5 fields of view of the tumor area per mouse. Data are shown as mean ± SEM. *$P \leq 0.05$, Student's *t* test. For CC3 staining, quantitation from staining signal was graphed as a ratio of the percentage of CC3+ cells to the percentage average of proliferating cells. Data are shown as mean ± SEM. Student's *t* test, NS. (**G**) Kaplan-Meier curve assessing survival of C57BL/6 albino mice (*n* = 10 per cohort) injected with either KPC control or KPC *Gdf-15*–knockdown cells.

was higher in *p65^{+/+}Ras* than in *p65^{-/-}Ras* MEFs (Figure 1C). These results indicate that *Gdf-15* expression in *Ras*-transformed cells is NF-κB dependent.

Next, we asked whether GDF-15 is necessary and sufficient for *p65^{+/+}Ras* MEFs to overcome the cytotoxic activity of activated macrophages. In a coculture system containing *p65^{+/+}Ras* MEFs and peritoneal macrophages, we observed that inhibiting GDF-15 activity with increasing doses of a GDF-15–neutralizing antibody led to a corresponding increase in cell death of *p65^{+/+}Ras* MEFs (Figure 1D). Conversely, the addition of increasing concentrations of recombinant GDF-15 progressively reduced the elimination of *p65^{-/-}Ras* MEFs by activated macrophages (Figure 1E). The purity of recombinant GDF-15 protein was confirmed by mass spectrometry (Supplemental Table 1), ruling out the possibility that protection of *p65^{-/-}Ras* MEFs was manifested by a contaminating fraction of TGF-β present in the recombinant protein preparation that we commercially obtained. Furthermore, growth of *p65^{+/+}Ras* MEFs or *p65^{-/-}Ras* MEFs was not altered by incubating cells with either the GDF-15 antibody or recombinant protein, suggesting that the effects of GDF-15 act directly on macrophages (Supplemental Figure 1, F and G). Together, these results imply that NF-κB regulation of GDF-15 in tumor cells is necessary and sufficient for evading macrophage-mediated killing.

GDF-15 promotes tumor development in vivo. To investigate whether GDF-15–mediated inactivation of macrophages plays a role in tumor development, we subcutaneously injected a mixture of *p65^{+/+}Ras* cells with either a neutralizing antibody against GDF-15 or IgG as control. Xenografts were performed in SCID mice, which maintain a functional innate immune system. Additional weekly intravenous injections of an anti–GDF-15 antibody or IgG were administered. Results showed delayed tumor development in mice that were given anti–GDF-15 antibody compared with IgG (Figure 1F). To determine whether GDF-15 specifically arising from tumor cells is important for this protection, we repeated the xenografts, this time with *p65^{+/+}Ras* MEF cells stably expressing a GDF-15 shRNA. Similar to antibody neutralization, the depletion of GDF-15 in *p65^{+/+}Ras* MEFs caused a delay in tumor development, as compared with shRNA control (Figure 1G and Supplemental Figure 1H). To substantiate these findings, we performed a gain-of-function experiment by injecting SCID mice with a mixture of *p65^{-/-}Ras* MEFs and recombinant GDF-15. An additional intravenous injection of recombinant protein was administered again after 1 week. Results showed that treating mice with GDF-15 trended toward accelerating tumor growth over that in saline controls (Supplemental Figure 1I). Taken together, these data support that GDF-15 confers a permissive environment for tumor development in vivo.

GDF-15 is required for the development of early pancreatic tumors. Having shown the tumor-promoting potential of GDF-15 in *Ras*-MEF cells, we next sought to validate our observations using a tumor model that better recapitulated human disease. A recently published study involving several types of cancers showed that circulating levels of GDF-15 are elevated in patients with pancreatic ductal adenocarcinoma (PDAC) (12). This finding was confirmed by measuring plasma GDF-15 levels from patients with PDAC compared with control subjects whose tissue was obtained from our own institutional pancreatic cancer tissue bank (Supplemental Figure 2A). Such data suggest that GDF-15 might be relevant in

pancreatic cancer development. Supporting this notion, RNA-seq analysis of tumor tissue from 183 PDAC cases from The Cancer Genome Atlas (TCGA) (http://genome-cancer.ucsc.edu) showed that patients with PDAC have higher *GDF-15* expression (Supplemental Figure 2B). In addition, we also evaluated survival data for patients suffering from PDAC obtained from TCGA and found a trend indicating that PDAC patients with elevated *GDF-15* expression have a poorer prognosis. This conclusion was also supported by a second data set (13) that revealed that PDAC patients with elevated *GDF-15* have a worse outcome compared with those with lower expression of *GDF-15* (Figure 2A). However, as is common in clinical studies, several patients from both data sets were censored, making it hard to evaluate statistical significance of the observed trends. Hence, we combined the 2 data sets, thereby increasing the power of the data, and found that PDAC patients with elevated *GDF-15* expression have significantly shorter survival times (Supplemental Figure 2C). Together, these data indicate a clinically relevant trend warranting preclinical studies to investigate the relevance of GDF-15 in pancreatic cancer development. To test this, we generated murine Panc02 pancreatic cancer cell lines stably expressing a GDF-15 shRNA (clones 12 and 15), which significantly silenced *Gdf-15* expression (Supplemental Figure 2D). These clones were cocultured with primary, peritoneal macrophages to determine whether GDF-15 was capable of neutralizing the antitumor activity of macrophages as we had observed with *p65^{+/+}Ras* MEFs. Similarly to what occurred in transformed MEFs, the level of cell death, as analyzed by flow cytometry staining for annexin V and 7-AAD, was higher in Panc02 cells lacking GDF-15 compared with control cells (Figure 2B and Supplemental Figure 2E). In addition, similar to MEF results, the growth rate of Panc02 cells was unaffected by silencing GDF-15 (Supplemental Figure 2F), demonstrating that the increased cell death in Panc02 cells lacking GDF-15 is not due to a proliferation defect, but rather an inability to neutralize the killing activity of peritoneal macrophages.

To determine whether these findings could be translated to a model of pancreatic cancer, we performed orthotopic injections of control and *Gdf-15*–knockdown Panc02 cells into the tail of the pancreas of immune-competent C57BL/6 mice. We observed that tumors from Panc02 control cells began to develop in the pancreas starting at 5 days after injection and continued to progress out to 14 days of observation (Figure 2C). In strong contrast, although tumors from Panc02 cells silenced for *Gdf-15* formed at 5 days, they were substantially smaller and remained smaller than control tumors out to the 14-day time point. Histological sections of tumors taken at 5, 10, and 14 days after injection showed that silencing *Gdf-15* decreased the number of proliferating tumor cells (Ki67^+) while increasing the number of apoptotic cells (cleaved caspase-3 [CC3]) relative to WT Panc02 tumors (Figure 2, D and E). Minimal numbers of Gr-1^+ (Ly6G) granulocytes were observed in cancerous lesions from *Gdf-15*–knockdown Panc02 and control Panc02 tumors (Supplemental Figure 2G), suggesting that infiltrating granulocytes contribute to only a very small fraction of cells present in the tumor microenvironment. We also observed that both the Panc02 and Panc02 tumors with *Gdf-15* knockdown are capable of activating stroma, as seen by staining for levels of α-SMA (Supplemental Figure 2H), suggesting that silencing *Gdf-15* does not affect stromal activation in the tumor.
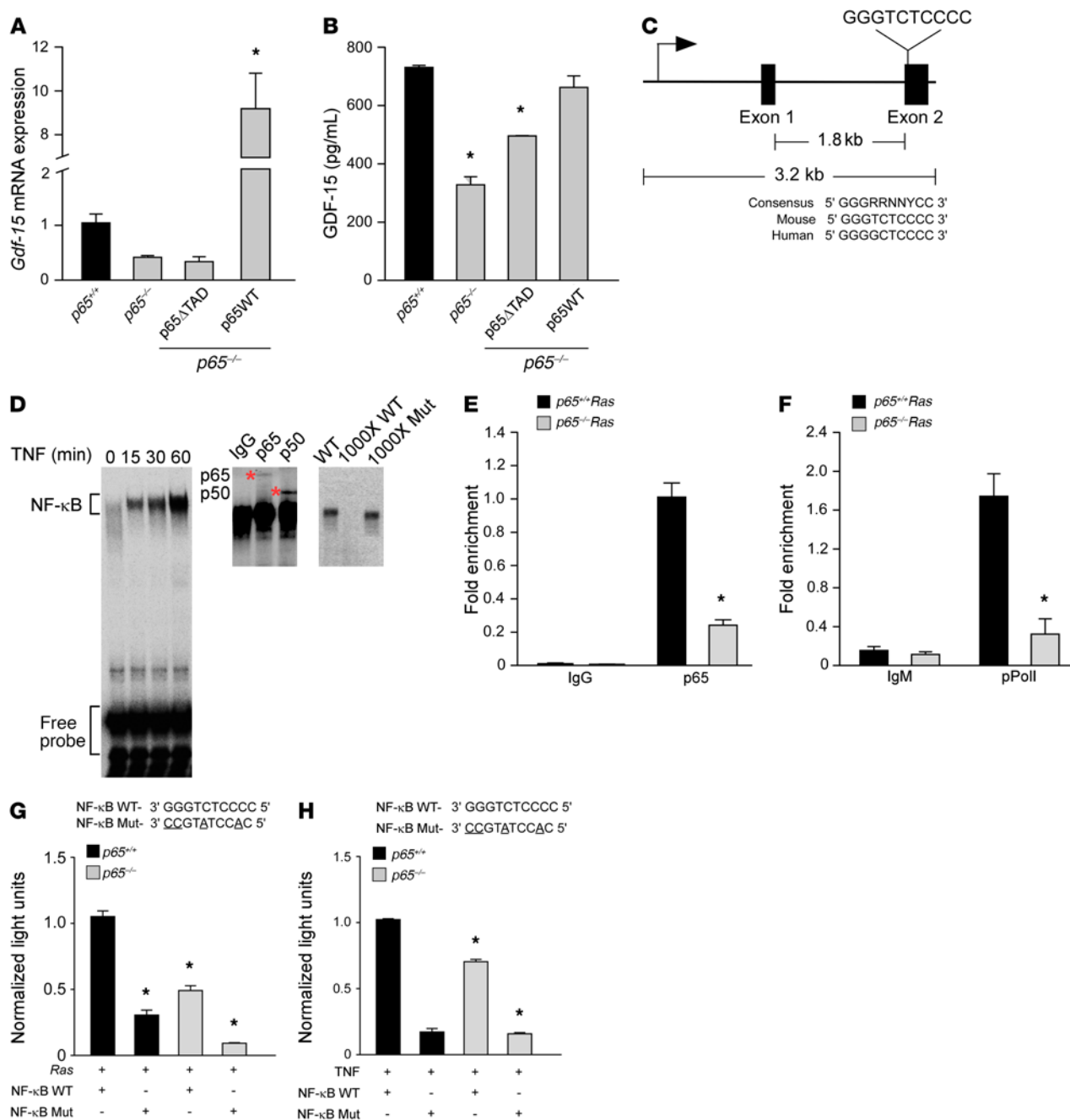
Figure 4. NF-κB is a direct regulator of Gdf-15. (A) $p65^{-/-}$ MEFs were infected with retrovirus for full-length (p65WT) or truncated p65 (p65ΔTAD). *Gdf-15* expression by qRT-PCR was assayed following TNF treatment (5 ng/ml) for 2 hours. *n* = 3. Data are shown as mean ± SEM. *P ≤ 0.005, 1-way ANOVA. **(B)** ELISA from conditioned media from transfected cells in **A**. *n* = 3. Data are shown as mean ± SEM. *P ≤ 0.05, 1-way ANOVA. **(C)** Schematic of *Gdf-15* gene with NF-κB consensus site in exon 2, compared with consensus site in mouse and human. **(D)** EMSA from TNF-treated *Ras* MEFs using NF-κB consensus site probe shown in **C**. Supershift assay from *Ras* MEFs incubated with antisera specific for p65 and p50. Asterisks indicate supershifted complexes. Specificity of the complexes was tested by adding ×1000 molar excess of labeled WT probe or nonlabeled mutant probe. **(E)** ChIP assays for p65 binding from *Ras* MEFs. DNA was amplified with oligonucleotides spanning the NF-κB site on exon 2 of *Gdf-15*. Fold enrichment over IgG controls (normalized to input) are indicated. *n* = 3. *P ≤ 0.05, Student's *t* test. **(F)** ChIP for pPol II (serine 2 version), as described in Figure 4E. DNA was amplified with the same oligonucleotides as shown in **E**. Fold enrichment over IgM controls (normalized to input) are indicated. *n* = 3. *P ≤ 0.05. Student's *t* test. **(G)** MEFs were transfected with a luciferase reporter with WT or mutated NF-κB consensus sites, as shown in **C**. Cells were cotransfected with H-Ras^{G12V}, and after 48 hours, luciferase activity was measured. *n* = 3. *P ≤ 0.05 compared with $p65^{+/+}$ MEFs with WT construct+ H-Ras, 2-way ANOVA. **(H)** MEFs were transfected with WT and mutant luciferase reporters and treated with 1 μl/ml of TNF for 2 hours. Luciferase activity was measured. *n* = 3. *P ≤ 0.05 when compared with $p65^{+/+}$ MEFs with WT construct with TNF, 2-way ANOVA.

One of the caveats of using Panc02 cells is their absence of the mutant *KRas* oncogene, which is mutated in 90% of PDAC patients (14). Therefore, we expanded our analysis generating additional *Gdf-15*–knockdown cell lines (clones 1 and 4) derived from *KRas*[G12D]; *p53*^{-/-}; *Pdx-Cre*^{+/-} (KPC) mice (15, 16) that also stably expressed a luciferase reporter gene that was used for bioluminescence imaging (17) (Figure 3A). KPC control or KPC *Gdf-15*–knockdown clones were then orthotopically injected into the tail of the pancreas of C57BL/6 albino mice, and tumor development was visualized. Similar to Panc02 results, mice injected with KPC cells knocked down for *Gdf-15* had considerably smaller tumors than control cells (Figure 3, B and C), a finding that was confirmed when orthotopic injections were repeated and tumor weights were measured as early as 5 days after injection (Figure 3D). Histological analysis revealed that control tumors contained a greater number of cells double-positive for Ki67 and the ductal marker CK-19 compared with the tumors obtained from *Gdf-15*–knockdown KPC cells (Figure 3, E and F). These same control tumor cells also exhibited a lower tendency to undergo apoptosis (Figure 3, E and F). Notably, mice with KPC tumors lacking GDF-15 survived longer compared with mice with control tumors (Figure 3G). Similar to results observed with the other cell lines, the ex vivo growth rate of KPC cells was unaffected by silencing GDF-15 (Supplemental Figure 3A). Taken together, our results indicate that GDF-15 plays an important role in the development of pancreatic cancer.
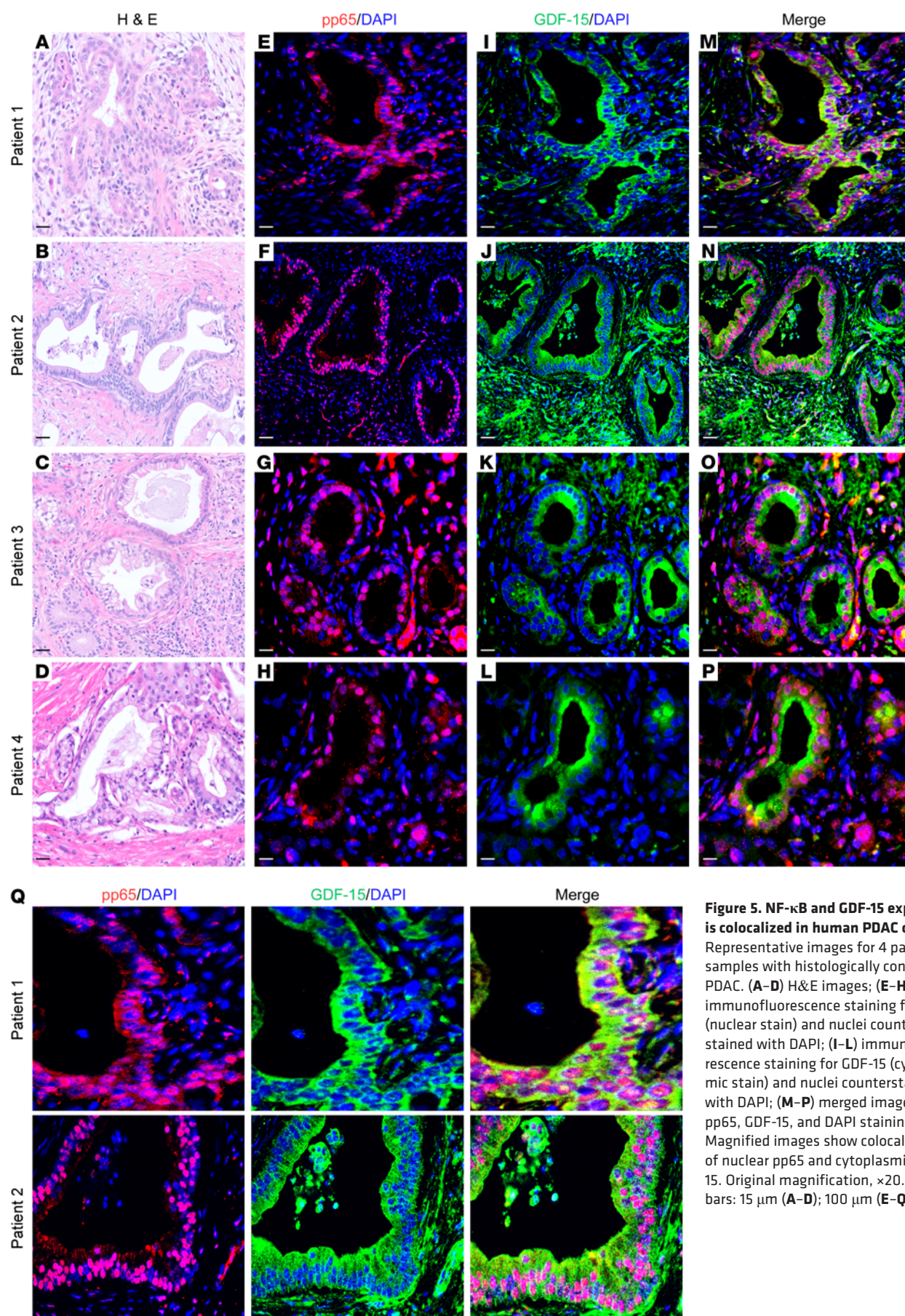
NF-κB is a direct regulator of Gdf-15. Having shown that GDF-15 is important for tumor development and survival of cancer cells against macrophage-mediated killing, we now sought to explore the mechanism of this regulation. We started by asking whether production of GDF-15 from tumor cells was under direct control of NF-κB. As shown earlier in Figure 1, B and C, and Supplemental Figure 1E, GDF-15 expression was reduced in MEFs lacking the p65 subunit, which drives NF-κB transcriptional activity. However, reconstitution of a full-length version of p65 (p65WT) restored *Gdf-15* mRNA and protein (Figure 4, A and B, and Supplemental Figure 4, A and B). In contrast, the reconstitution of a truncated version of p65 lacking the transactivation domain (p65ΔTAD) was unable to rescue *Gdf-15* expression in *p65*^{-/-} MEFs. Thus, the transcriptional activity of NF-κB is necessary to produce GDF-15. Next, we searched by rVista for NF-κB consensus binding sites throughout the *Gdf-15* gene. A site conserved between mice and humans was located in exon 2 (Figure 4C). EMSAs performed with the predicted consensus sequence and extracts from TNF-stimulated *p65*^{+/+}*Ras* MEFs showed NF-κB binding (Figure 4D). Furthermore, super-shift analysis showed that these NF-κB complexes contained the p65 and p50 subunits, and competition EMSAs confirmed the specificity of these complexes (Figure 4D). ChIP assays verified p65 binding on exon 2 of *Gdf-15*, which was higher in *p65*^{+/+}*Ras* MEFs compared with the *p65*^{-/-}*Ras* MEFs (Figure 4E). Binding of p65 also corresponded to enhanced occupancy of phosphorylated RNA polymerase II (pPol II, which is phosphorylated on serine 2) (Figure 4F), suggesting that the binding of p65 to exon 2 of *Gdf-15* promotes active transcription. To further substantiate these findings, we constructed a luciferase reporter plasmid containing the NF-κB–binding element from exon 2 of *Gdf-15*. Results showed that GDF-15 reporter activity was enhanced in *p65*^{+/+}*Ras* MEFs and in cells stimulated by TNF (Figure 4, G and

H). Importantly, this activity diminished when similar assays were repeated with a luciferase reporter containing a mutation in the NF-κB consensus site from exon 2 of *Gdf-15*. Collectively, these data demonstrate that *Gdf-15* is a direct transcriptional target of NF-κB.

NF-κB and GDF-15 are coexpressed in tumor cells of patients with PDAC. Given that GDF-15 levels are elevated in pancreas tumors and, as we showed, required for pancreatic tumor development in mice, we explored whether the regulation of *Gdf-15* by NF-κB was relevant in PDAC patients. Dual immunofluorescence staining using antibodies recognizing GDF-15 and the activated form of p65 (pp65) showed clear evidence of colocalization in epithelial cells lining the pancreatic ducts in 9 patients with PDAC (Figure 5 and Supplemental Figure 5A). Specifically, pp65 staining was localized to the nuclei of ductal epithelial cells, while GDF-15 expression predominated in the cytoplasm of these cells. Although GDF-15 expression was also present in the surrounding stromal compartment, little colocalization was observed with pp65, suggesting that the majority of GDF-15 regulation by NF-κB is specific to pancreatic ductal epithelial cells. To verify that regulation of GDF-15 by NF-κB occurs in pancreatic cancer cells, we utilized CRISPR-Cas9 gene editing to generate a KPC cell line lacking p65 (KPC Δp65[CRISPR]), which we confirmed at both the DNA and protein levels (Supplemental Figure 5, B and C). Compared with control cells, KPC Δp65[CRISPR] had a pronounced reduction in *Gdf-15* expression (Supplemental Figure 5D). Together, these data suggest that increased GDF-15 in PDAC patients derives largely from pancreatic epithelial tumor cells and that such expression is under the control of NF-κB.

GDF-15 suppresses macrophage cytotoxic activity by inhibiting the production of TNF and iNOS. Having demonstrated that GDF-15 production from PDAC cells is under direct control of NF-κB, we next explored the mechanism by which GDF-15 suppresses the antitumor activity of inflammatory macrophages. Recent reports indicate that macrophages participate in immune surveillance in the early phases of pancreatic cancer (4). To confirm this notion, we subcutaneously injected KPC cells silenced for *Gdf-15* and then performed an intraperitoneal injection of clodronate liposomes, which function to deplete circulating monocytes, into C57BL/6 mice. Results showed that tumor development was enhanced in clodronate liposome–treated mice compared with the controls (Figure 6A). As an additional control, we also treated C57BL/6 mice subcutaneously injected with KPC control cells. Consistent with the function of macrophages to switch to assisting tumor growth during the progressive phase of tumor development, KPC tumors were significantly reduced in the clodronate-treated group (Supplemental Figure 6A). Together, these data support the hypothesis that macrophages possess antitumor activity in the development of pancreatic cancer and that macrophages are at least one of the cell types targeted by GDF-15 during early tumor development.

Work from our laboratory and others have shown that macrophages mediate their killing activity through secretion of the proapoptotic factors TNF and NO (10, 18). To confirm this in pancreatic tumor cells, we treated KPC Δp65[CRISPR] cells with TNF or the NO donor SNP. Both treatments induced strong cell killing compared with KPC vector control cells (Figure 6, B and C). No killing was seen when similar treatments were performed with macrophage-producing cytokines IFN-β-1, IL-12, or IL-15 (Sup-

Figure 5. NF-κB and GDF-15 expression is colocalized in human PDAC cells. (A) Representative images for 4 patient samples with histologically confirmed PDAC. (**A–D**) H&E images; (**E–H**) immunofluorescence staining for pp65 (nuclear stain) and nuclei counterstained with DAPI; (**I–L**) immunofluorescence staining for GDF-15 (cytoplasmic stain) and nuclei counterstained with DAPI; (**M–P**) merged images of pp65, GDF-15, and DAPI staining. (**Q**) Magnified images show colocalization of nuclear pp65 and cytoplasmic GDF-15. Original magnification, ×20. Scale bars: 15 μm (**A–D**); 100 μm (**E–Q**).

plemental Figure 6, C–E). However, KPC Δp65^{CRISPR} cells were moderately affected when treated with ROS (Supplemental Figure 6B), indicating that KPC cells are sensitive to ROS and further suggesting that p65 may be regulating endogenous mechanisms to protect these cells from ROS-mediated cell death. Therefore, as previously demonstrated with other cell types (10), pancreatic cancer cells appear to utilize NF-κB to suppress the surveillance of macrophages, mainly by resisting the cytotoxic effects of TNF and NO. To determine whether this resistance to macrophage activity is mediated through GDF-15, we performed cocultures with KPC *Gdf-15*–knockdown cells and peritoneal macrophages that were either WT or genetically ablated for *Tnf* and *iNOS* alleles (Tnf iNOS double-knockout mice, herein referred to as DKO; iNOS is the major enzyme responsible for the production of NO in macrophages). Results showed that, while KPC control cells were resistant to WT macrophages, KPC cells lacking GDF-15 were more sensitive to WT macrophage–mediated killing (Figure 6, D and E). The killing activity in KPC cells lacking GDF-15 was markedly reduced, albeit not completely, when these cells were cultured with DKO macrophages. The incomplete rescue of DKO macrophage–mediated killing implies that other factors, perhaps ROS, may be involved in mediating this killing activity. However, since GDF-15 protected KPC cells from macrophage-mediated killing, these data indicate that GDF-15 is needed by pancreatic cancer cells to suppress the proapoptotic activity of macrophages, derived through TNF, NO, and likely ROS.

To determine whether macrophage suppression by GDF-15 occurs in vivo, we injected *p65*^{+/+}*Ras* cells silenced for GDF-15 into the peritoneum of SCID mice and then measured by flow cytometry the number of F4/80⁺ macrophages expressing TNF. Results showed that whereas only 26% of macrophages expressed TNF after the injection of control cells, injection of *p65*^{+/+}*Ras* cells silenced for GDF-15 led to the recruitment of 46% of macrophages positive for TNF (Figure 6F and Supplemental Figure 6F). A similar difference in TNF⁺ macrophages was observed following the peritoneal injection of Panc02 cells knocked down for GDF-15 expression (Figure 6G and Supplemental Figure 6F). To confirm these findings, we stained orthotopic Panc02 tumor sections 5 days after tumor cell injection for F4/80 and TNF. Results showed that Panc02 tumors exhibited fewer F4/80⁺; TNF⁺ macrophages compared with the Panc02 tumors with *Gdf-15* knockdown (Figure 6H, Supplemental Figure 6G, and Supplemental Video 1). In comparison, no differences were detected for the granulocyte cell marker Gr-1 (Ly6G) (Supplemental Figure 2G), demonstrating that the effect of GDF-15 activity was specific to macrophages in these tumors. Importantly, when results were verified with KPC tumors lacking GDF-15, a similar increase in F4/80⁺; TNF⁺ macrophages was observed compared with that in control tumors (Figure 6I). Together, these data suggest that GDF-15 suppresses the antitumor activity of inflammatory macrophages by limiting the production of proapoptotic factors, such as TNF and NO.

GDF-15 signals in macrophages to suppress NF-κB signaling via TAK-1. To probe into the mechanism by which GDF-15 inhibits macrophage production of TNF and NO, we treated RAW264.7 macrophages or primary bone marrow–derived macrophages with recombinant GDF-15 and measured gene expression of *Tnf* and *iNOS*. Results showed that GDF-15 strongly reduced the expression of

both genes (Figure 7A and Supplemental Figure 7A). Since *Tnf* and *iNOS* are well-established NF-κB target genes (19, 20) we queried whether GDF-15 induced the suppression of these factors by inhibiting NF-κB. Consistent with this notion, ChIP analyses revealed that p65 occupancy on both *Tnf* and *iNOS* promoters was strongly reduced in response to GDF-15 treatment in RAW264.7 cells (Figure 7B). These data suggest that GDF-15 suppression of TNF and NO occurs via the inhibition of NF-κB. Taken together, our results reveal that while NF-κB is responsible for the synthesis and secretion of GDF-15 from pancreatic tumor cells, GDF-15 inhibits NF-κB activity in macrophages to overcome immune surveillance.

Finally, we analyzed how GDF-15 inhibits NF-κB in macrophages. Limited evidence exists that GDF-15 signals through the canonical TGF-β receptor and pathway (21–23). Phospho-SMAD2 and -3 (pSMAD2 and pSMAD3) mediate activation of canonical TGF-β signaling while the noncanonical pathway of TGF-β signals through the activation of phosphorylated TGF-β–activated kinase (pTAK1), leading to further downstream activation of NF-κB or the p38 MAP kinase (24, 25). Consistent with these findings, we observed that treatment of RAW264.7 macrophages with GDF-15 increased the levels of pSmad2 and pSmad3 (Supplemental Figure 7B). However, in contrast to the typical noncanonical activation of TAK1 in response to TGF-β, GDF-15 treatment of RAW264.7 and primary bone marrow macrophages led to a steady decline in TAK1 activity (Figure 7C and Supplemental Figure 7C). Active TAK1 stimulates the IκB kinase (IKK) complex that in turn signals to classical NF-κB and the p65 subunit (25). However, in GDF-15–treated macrophages, IKK kinase activity was also reduced, as measured by decreasing levels of phospho-IκB protein (pIκBα; Figure 7D). In comparison with suppression of NF-κB, GDF-15 treatment had minimal effects on p38 activity (pp38; Supplemental Figure 7D). Therefore, although GDF-15 signaling in macrophages resembles the canonical TGF-β pathway, its signaling is distinct from the noncanonical TGF-β pathway in macrophages, acting instead to repress TAK1 and NF-κB target genes. Together, these data support the concept that NF-κB induces GDF-15 expression in tumor cells, which upon its secretion, neutralizes the cytotoxic activity of infiltrating macrophages through inhibition of the TAK1/IKK/NF-κB pathway and downstream production of TNF and NO.

Discussion

Constitutive activation of NF-κB in cancer cells is believed to contribute to functions intrinsic to the tumor cell, regulating genes that promote cell survival, proliferation, migration, and the epithelial-to-mesenchymal transition (9). In contrast, much less is known about the cell-extrinsic functions of NF-κB that influence tumor development, specifically with regard to the stroma within the tumor microenvironment. In this study, we describe such an interaction between tumor cells and host macrophages, revealing a feature of NF-κB during tumorigenesis. Our findings support a model illustrated in Figure 7E, in which activated macrophages function in immune surveillance by secreting cytotoxic factors TNF and NO. Tumor cells are able to overcome this macrophage-killing activity by utilizing NF-κB to promote the expression of GDF-15. Secreted GDF-15 inactivates tumor-infiltrating macrophages by negatively regulating TAK1, which in turn causes NF-κB activity to be downregulated, leading to the
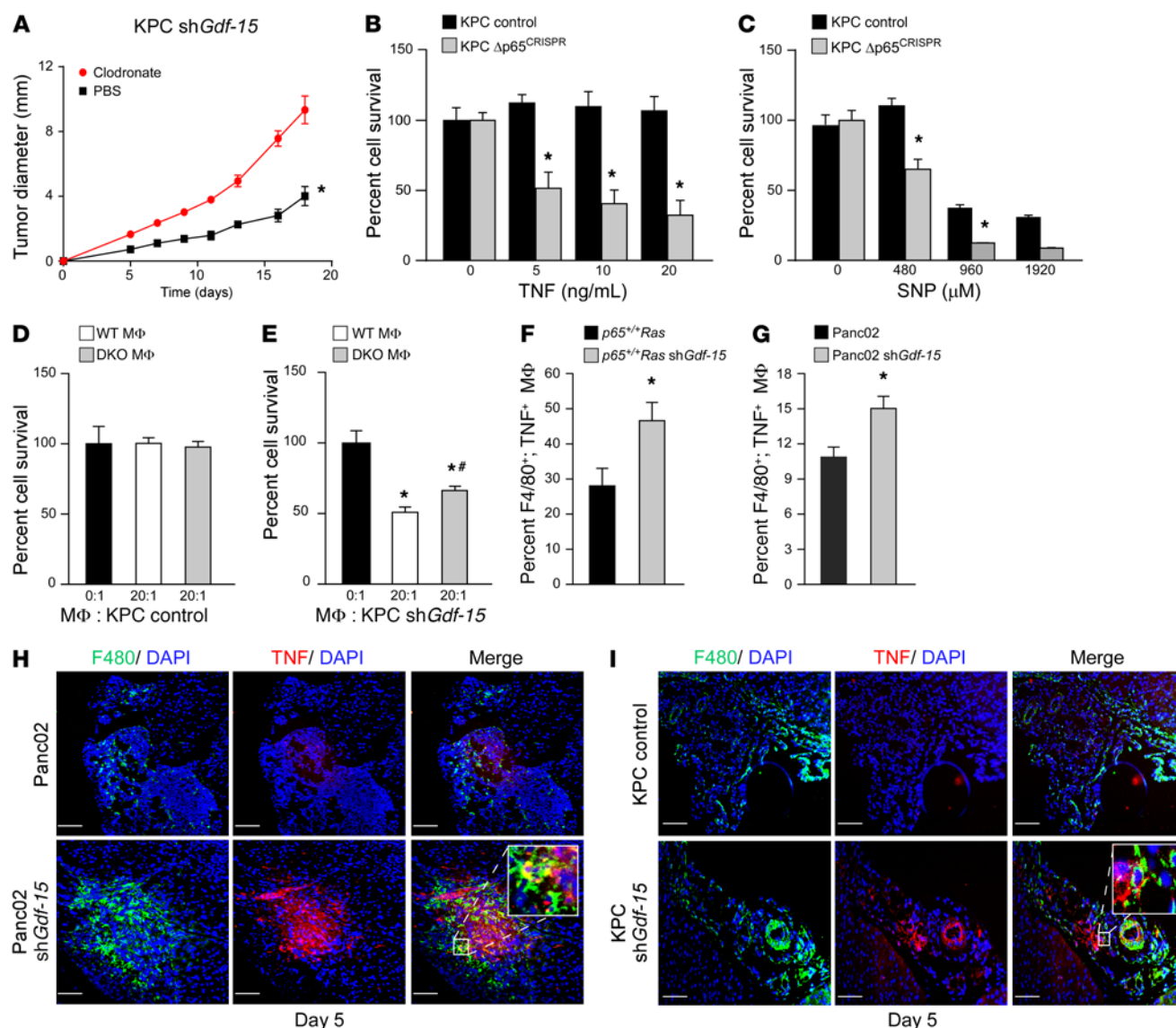
Figure 6. GDF-15 suppresses macrophage cytotoxicity by inhibiting TNF. (**A**) KPC *Gdf-15*–knockdown cells were injected into mice and treated with clodronate liposomes or control liposomes biweekly. Tumor sizes were measured. *n* = 5 per cohort. Data are shown as mean ± SEM. *P ≤ 0.05, SPSS repeated measures, general linear model. (**B** and **C**) MTS assay following TNF and SNP treatment of KPC control and Δp65^{CRISPR} cells. Data represent the mean of 2 independent experiments performed in triplicate. *P ≤ 0.05, 2-way ANOVA. (**D** and **E**) KPC control and *Gdf-15*–knockdown cells were cocultured with WT or *Tnf* and *iNOS* DKO macrophages. Graph represents cell survival. *n* = 6. Data are shown as mean ± SEM. *P ≤ 0.05 compared with 0:1; #P ≤ 0.05 compared with 20:1 WT macrophages, 1-way ANOVA. (**F**) *Ras* MEFs knockdown for *Gdf-15* were injected into SCID mice, and macrophages were harvested and analyzed by FACS for F4/80+ and TNF+. Graph represents mean ± SEM of F4/80+; TNF+ double-positive cells from 6 mice in 2 independent experiments. *P ≤ 0.05, Student's *t* test. (**G**) FACS analysis similar to **F** performed on SCID mice (*n* = 5 for each group) following intraperitoneal injections with Panc02 control and *Gdf-15*–knockdown cells. Graph represents mean ± SEM of F4/80+; TNF+ double-positive macrophages. *P ≤ 0.05, Student's *t* test. (**H**) Immunohistochemistry on tumors following injections of Panc02 control and *Gdf-15*–knockdown cells. Tumors were harvested, sectioned, and stained for F4/80 and TNF and nuclei counterstained with DAPI. Inset represents magnified image of F4/80+, TNF+ macrophages in *Gdf-15*–knockdown Panc02 tumors. (**I**) Tumors harvested from KPC control and *Gdf-15* shRNA–injected C57BL/6 albino mice 5 days after injection were sectioned and stained in the same way as the Panc02 cells. Inset represents magnified image of F4/80+, TNF+ macrophages in *Gdf-15*–knockdown KPC tumors. Original magnification, ×20. Magnification in insets ×20. Scale bar: 100 μm.

further downregulated expression of NF-κB target genes *Tnf* and *iNOS*. In the absence of TNF and NO, macrophages are no longer able to eliminate tumor cells, thus allowing the expansion of a developing tumor. Although less clear, our data also indicate that GDF-15 protects tumor cells from ROS-mediated toxicity, which is included in the model, but will require further testing and validation with genetic studies.

Since macrophages participate in immune surveillance (2), our model argues that regulation of GDF-15 by NF-κB might be relevant during the early stages of tumor development. How NF-κB functions during these early events has not been as well studied in comparison with the role of NF-κB in later stages of tumor progression (26). However, recent findings provided insight on the potential functions of NF-κB in tumor initiation.
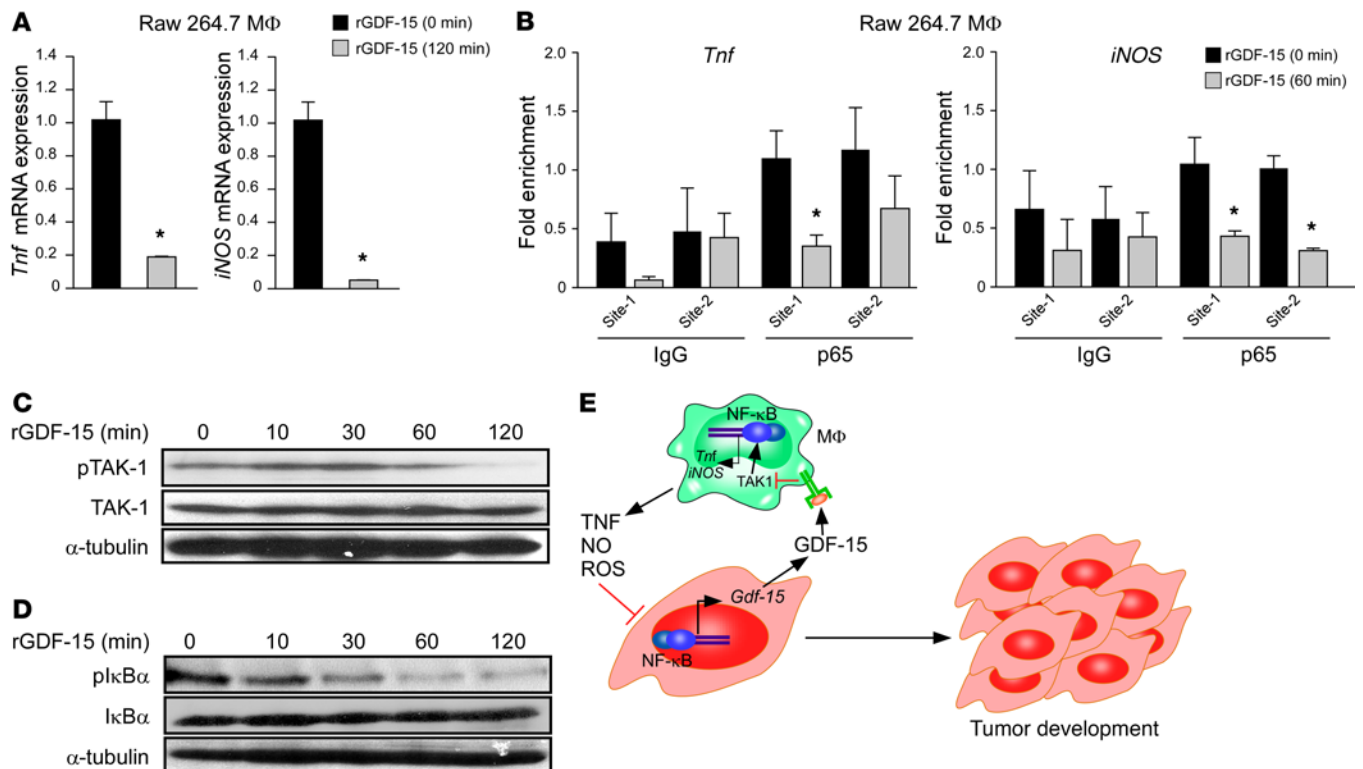
Figure 7. GDF-15 signals in macrophages to suppress NF-κB signaling via TAK1. (A) Raw 264.7 macrophages were treated with 5 ng/ml of rGDF-15 for 120 minutes, and then *Tnf* and *iNOS* expression was quantitated by qRT-PCR. *n* = 3. *$P ≤ 0.05$, Student's *t* test. (**B**) ChIPs were performed on chromatin from Raw 264.7 macrophages treated with rGDF-15 for 60 minutes. Precipitated DNA was amplified with oligonucleotides spanning each of the 2 NF-κB consensus sites on the promoters of the respective *Tnf* and *iNOS* genes. Fold enrichment over IgG controls and normalized to input are indicated. *n* = 3 each. *$P ≤ 0.05$, Student's *t* test. (**C**) Western blot was performed from Raw 264.7 macrophages treated with 5 ng/ml rGDF-15, and cell lysates were probed for pTAK1 and total TAK1. α-Tubulin was used as a loading control. (**D**) Similar to **C**, except that cell lysates were probed for IκBα phosphorylation and total IκBα with α-tubulin served as a loading control. (**E**) A model for how NF-κB regulates macrophage immune surveillance through GDF-15. The diagram shows that tumor cells utilize NF-κB for protection against infiltrating macrophages. Macrophages mediate this surveillance response through the secretion of proapoptotic factors TNF, NO, and ROS, but tumor-derived NF-κB overcomes these proapoptotic factors by synthesizing and secreting GDF-15, which signals in macrophages to suppress the production of TNF and NO, in turn inhibiting NF-κB signaling in the macrophages.

Schwitalla and colleagues proposed that NF-κB participates in the initiation of colon cancer by maintaining the stemness of the crypt cells as a way to form a reservoir of tumor-initiating cells (27). Investigators further used an inflammation-induced model of colon cancer to show that stromal fibroblast–derived NF-κB secretes IL-6 to activate STAT3 in epithelial cells to promote their proliferation (28). In our own laboratory, we used an MEF model of senescence to show that NF-κB is capable of exhibiting different oncogenic properties based on the staging of an initiating tumor. In preneoplastic cells, the p65 subunit of NF-κB functions as a tumor suppressor by maintaining cells in senescence (29). In this model, maintenance of senescence was associated with a more stable genome that p65 controlled through its involvement in DNA repair in response to genotoxic stress during the senescent condition (29). Furthermore, following the loss of tumor suppressors and escape from senescence, expression of oncogenic *Ras* causes p65 to switch its function to a tumor promoter to protect transformed cells against immune surveillance (10). This concept of NF-κB switching from a tumor suppressor to tumor promoter during an early phase of tumorigenesis was recently supported in a genetically engineered mouse model of pancreatic cancer (30), but the mechanism by which NF-κB was able to over-come immune surveillance in the initiating stages of tumor development had not been resolved.

Tumor-infiltrating macrophages can have both tumor-eliminating and tumor-promoting functions. Macrophages are well established as facilitating tumor progression (31), but evidence also indicates that prior to becoming tumor-associated macrophages (TAMs), these cells participate in antitumor responses, similar to what we describe in our current study. More recent results reveal that treating both murine and human pancreatic cancers with a CD40 agonist leads to tumor regression and increases the efficiency of chemotherapy by improving macrophage activation (4). Clodronate liposome–mediated depletion of macrophages has also been shown to accelerate tumor formation in a xenograft tumor model (10), a finding we also showed in this study, which supports the idea that inflammatory macrophages participate in early tumor immune surveillance. At least with respect to the surveillance property of macrophages, our current results indicate that NF-κB is able to modulate this function through direct regulation of GDF-15. We modeled this function of NF-κB primarily in pancreatic cancer because NF-κB is constitutively activated in this tumor type (32–34) and there is substantial evidence in pancreatic cancer that supports the involvement of

a dense stroma with infiltration of innate immune cells (35, 36). In addition, GDF-15 is highly expressed in PDAC compared with other cancers (12). However, interest in this cytokine has been mostly restricted to its role as a potential biomarker, and therefore no mechanism has been proposed for how this cytokine might function during the development of PDAC. Our data suggest that the elevation of GDF-15 in the circulation of PDAC patients derives from the activation of the p65 subunit of NF-κB in malignant ductal epithelial cells, since GDF-15 was also found to colocalize in these same cells in PDAC cases, and we further identified *Gdf-15* as a direct transcriptional target of NF-κB. Mechanistically, our orthotopic data showed that knocking down *Gdf-15* in Panc02 and KPC cells delayed the formation of pancreatic tumors and increased overall survival in mice, which correlated tightly with the increase in macrophages expressing TNF. Thus, adhering to our model, we propose that *Gdf-15* is directly regulated by NF-κB in the early phases of pancreatic cancer development to circumvent the immune surveillance activity of infiltrating inflammatory macrophages. We do not believe that this role for NF-κB and GDF-15 is limited to pancreatic cancer, since immune surveillance is considered a general feature of tumorigenesis (3) and numerous cancer types depend on the constitutive activation of NF-κB (9). Although levels of GDF-15 have also been shown to be elevated in prostate cancer, the function of GDF-15 in this cancer type is unclear, as both tumor-promoting and tumor-suppressing activities are associated with this cytokine (37).

In addition to identifying *Gdf-15* as an NF-κB transcriptional target, our study also sheds light on the mechanism by which GDF-15 signals in macrophages. Although GDF-15 bears some structural redundancy with other TGF-β family members that can activate canonical SMAD2/3 signaling, the ability of GDF-15 to inhibit NF-κB through TAK1 inactivation highlights the divergent signaling of GDF-15 from other TGF-β family members. Also revealing is the ability of GDF-15 to inhibit TAK1, which appears specific to IKK/NF-κB signaling, since only a minimal effect was seen on the other TAK1 target, p38. Furthermore, GDF-15–mediated IKK suppression and subsequent NF-κB inhibition led to decreased expression of TNF and NO. While our study shows that GDF-15 can inhibit TAK1 activation, the signaling mechanism that leads to TAK1 inactivation remains to be resolved. Based on the differences in the timing of the signaling between activation of the canonical TGF-β pathway and inactivation of TAK1 (Supplemental Figure 7B and Figure 7C), we speculate that inhibition of TAK1 could be occurring at the level of the TGF-β receptor, a possibility that will need to be tested in subsequent studies. Also, TAK1 is a central node of NF-κB activation, not just via TGF-β signaling, but also through other signaling pathways such as the TNF receptor. Hence, it is possible that GDF-15 may be signaling via more than one receptor and inhibition of TAK1 may be occurring through multiple mechanisms. Taken together, our results reveal the complex activities of NF-κB during tumor development. While tumor-associated activity of NF-κB is required to overcome macrophage surveillance, GDF-15–mediated inhibition of NF-κB signaling in infiltrating macrophages blocks the antitumor immune response. To the best of our knowledge, this type of NF-κB–arbitrated regulatory loop between tumor and immune cell is the first to be described with relevance to pancreatic cancer.

Methods

Cell lines. *p65+/+* and *p65–/–Ras* MEFs and *p65+/+* and *p65–/–* MEFs were maintained as described previously, cultured in DMEM with 10% FBS (10, 29). Panc02 (provided by T. Williams, OSU) cells were cultured in RPMI with 10% FBS, and Raw 264.7 cells were cultured on sterile nontissue culture dishes using RPMI with 5% FBS. KPC luciferase cell lines (provided by Z. Cruz-Monserrate, OSU) were cultured in DMEM with 10% FBS.

Coculture and cell-survival assays. *p65+/+* and *p65–/–Ras* MEFs were cocultured with primary peritoneal macrophages (20:1) in 100 μl of medium with heat-inactivated FBS in a 96-well plate. After 48 hours, cells were trypsinized and surviving cells counted by a trypan blue exclusion assay. Control conditions contained MEF cells alone without macrophages. Isolation of peritoneal macrophages was done as previously described (10). 1 ml of Brewer's thioglycolate medium was injected intraperitoneally into the mice at about 8 weeks of age. Peritoneal cells were then isolated using DMEM with 10% heat-inactivated FBS after about 4 to 5 days. These cells were cultured for 3 hours and, after 2 rounds of trypsinization and washing to remove nonadherent or loosely adherent cells, adherent macrophages (>90%) were harvested and resuspended. For cell-survival assays using the Panc02 cells and the Panc02 shGDF-15 cells, cocultures were carried out in 35-mm dishes using a 2:1 ratio of macrophages to cancer cells. After incubating for 48 hours, cells were harvested and stained with FITC-conjugated rat anti-mouse CD11b (BioLegend, clone M1/70) and then washed with annexin V buffer. This was followed by staining with annexin V and 7-AAD using the Phycoerythrin–Annexin V Staining Kit (BD Biosciences — Pharmingen, catalog 559763), and then the cells were analyzed using Flowsight 2 Imaging flow cytometry. Murine spleen cells were used to run isotype controls to determine the specificity of the CD11b antibody.

Orthotopic tumor implantation. Panc02 or Panc02 sh*Gdf-15* cells and KPC control or KPC sh*Gdf-15* (1×10^5) were suspended in a 40 μl mixture of Matrigel (Sigma-Aldrich) and subsequently injected into the tail of the pancreas using a survival surgery procedure described previously (38) on age-matched C57BL/6 and C57BL/6 albino female mice, respectively, of approximately similar weight. Control mice cohorts were injected with Matrigel alone. Tumor measurements were made by harvesting and weighing the pancreas at the designated time points. Final tumor weights were calculated by normalizing to weights of the Matrigel-injected control pancreas using the following formula: tumor weight = weight of pancreas with tumor – average weight of Matrigel-injected pancreas. In the cases of the KPC orthotopic tumors, bioluminescence imaging was done by injecting 15 mg/ml of D-luciferin solution (Sigma-Aldrich) in PBS intraperitoneally into the mice that were subsequently imaged on a PerkinElmer IVIS Illumina-II Imaging system. Differences in bioluminescence of the KPC control and KPC sh*Gdf-15* cells were established as described previously (39) using serially diluted numbers of the cells (1×10^6 to 1×10^2) and estimating differences in slopes between the 2 standard curves by linear regression analysis. It was established by bioluminescence imaging that KPC cells knocked down for *Gdf-15* were approximately 6 times more luminescent than control cells and hence ROI calculations were used to compensate for the difference.

Patients. Blood samples were obtained at time of surgery from men and women with suspected PDAC, which was histologically confirmed in resected tumors or metastases. Patients receiving preoperative chemotherapy were excluded from the analysis. Patients utilized as con-

trol subjects were undergoing abdominal surgery for other conditions and were not suspected to have cancer. GDF-15 was measured with a standard ELISA (R&D Systems, catalog SGD150). Samples were analyzed in duplicate. For localization of GDF-15 and activated NF-κB, a subset of resected tumors from the above patients were formalin fixed, paraffin embedded, and subsequently stained for phosphorylated p65 and GDF-15 and visualized using immunofluorescence.

For further information, see Supplemental Methods.

RNA-seq analysis. All original RNA-seq analysis data were deposited in the NCBI's Gene Expression Omnibus (GSE101092).

Statistics. ANOVA was adopted to analyze differences between groups in experiments in which more than 2 groups were compared at a single time, including tumor growth studies. Correlation repeated measure was utilized to analyze differences in tumor growth. Two-tailed Student's *t* tests were used for analyzing all other experiments. Kaplan-Meier analysis was used in animal survival studies. Statistical software, such as GraphPad Prism and SPSS (IBM), was used for all analysis. A *P* value less than or equal to 0.05 was considered significant for all statistical analysis.

Study approval. Our laboratory received approval from the OSU IRB for use of human tissue specimens for research. All patients in our study provided prior written consent to participate in the study. We also received approval on the use of mice for all the procedures used in this study from the OSU IACUC. All procedures employed in this study conform to the regulations put forth by the respective IRBs.

Author contributions

NMR designed, performed, and analyzed the experiments with guidance from DJW and DCG. JMP performed the bioinformatics analysis from the RNA-seq data set. EET assisted with patient studies, and BJS evaluated the histopathology of human tissues. KJL generated CRISPR clones. PVR and EH procured and processed patient tissue and serum samples. CRS and MED provided the human specimens. RDK optimized and performed the immunohistochemistry staining of mouse tumor tissues. TMW provided expertise and contributed to the analysis related to pancreatic cancer. GWL provided expertise on tumor development and assisted with the writing of the manuscript. DJW and DCG conceptualized the project and contributed to the writing and editing of the manuscript. DCG supervised the project. All authors reviewed and approved the manuscript.

1. Hanahan D, Weinberg RA. The hallmarks of cancer. *Cell*. 2000;100(1):57–70.
2. Ribatti D. The concept of immune surveillance against tumors. The first theories. *Oncotarget*. 2017;8(4):7175–7180.
3. Colotta F, Allavena P, Sica A, Garlanda C, Mantovani A. Cancer-related inflammation, the seventh hallmark of cancer: links to genetic instability. *Carcinogenesis*. 2009;30(7):1073–1081.
4. Beatty GL, et al. CD40 agonists alter tumor stroma and show efficacy against pancreatic carcinoma in mice and humans. *Science*. 2011;331(6024):1612–1616.
5. Davies LC, Jenkins SJ, Allen JE, Taylor PR. Tissue-resident macrophages. *Nat Immunol*. 2013;14(10):986–995.
6. Woo SR, Corrales L, Gajewski TF. Innate immune recognition of cancer. *Annu Rev Immunol*. 2015;33:445–474.
7. Oh H, Ghosh S. NF-κB: roles and regulation in different CD4(+) T-cell subsets. *Immunol Rev*. 2013;252(1):41–51.
8. Hayden MS, Ghosh S. Shared principles in NF-kappaB signaling. *Cell*. 2008;132(3):344–362.
9. Xia Y, Shen S, Verma IM. NF-κB, an active player in human cancers. *Cancer Immunol Res*. 2014;2(9):823–830.
10. Wang DJ, Ratnam NM, Byrd JC, Guttridge DC. NF-κB functions in tumor initiation by suppressing the surveillance of both innate and adaptive immune cells. *Cell Rep*. 2014;9(1):90–103.
11. Bootcov MR, et al. MIC-1, a novel macrophage inhibitory cytokine, is a divergent member of the TGF-beta superfamily. *Proc Natl Acad Sci U S A*. 1997;94(21):11514–11519.
12. Wang X, et al. Macrophage inhibitory cytokine 1 (MIC-1/GDF15) as a novel diagnostic serum biomarker in pancreatic ductal adenocarcinoma. *BMC Cancer*. 2014;14:578.
13. Moffitt RA, et al. Virtual microdissection identifies distinct tumor- and stroma-specific subtypes of pancreatic ductal adenocarcinoma. *Nat Genet*. 2015;47(10):1168–1178.
14. Hezel AF, Kimmelman AC, Stanger BZ, Bardeesy N, Depinho RA. Genetics and biology of pancreatic ductal adenocarcinoma. *Genes Dev*. 2006;20(10):1218–1249.
15. Torres MP, Rachagani S, Souchek JJ, Mallya K, Johansson SL, Batra SK. Novel pancreatic cancer cell lines derived from genetically engineered mouse models of spontaneous pancreatic adenocarcinoma: applications in diagnosis and therapy. *PLoS ONE*. 2013;8(11):e80580.
16. Reznik R, Hendifar AE, Tuli R. Genetic determinants and potential therapeutic targets for pancreatic adenocarcinoma. *Front Physiol*. 2014;5:87.
17. Ma Y, Hwang RF, Logsdon CD, Ullrich SE. Dynamic mast cell-stromal cell interactions promote growth of pancreatic cancer. *Cancer Res*. 2013;73(13):3927–3937.
18. Keller R, Keist R, Wechsler A, Leist TP, van der Meide PH. Mechanisms of macrophage-mediated tumor cell killing: a comparative analysis of the roles of reactive nitrogen intermediates and tumor necrosis factor. *Int J Cancer*. 1990;46(4):682–686.
19. Shakhov AN, Collart MA, Vassalli P, Nedospasov SA, Jongeneel CV. Kappa B-type enhancers are involved in lipopolysaccharide-mediated transcriptional activation of the tumor necrosis factor alpha gene in primary macrophages. *J Exp Med*. 1990;171(1):35–47.
20. Morris KR, Lutz RD, Choi H, Kamitani T, Chmura K, Chan ED. Role of the NF-κB signaling pathway and kB cis-regulatory elements on the IRF-1

and iNOS promoter regions in mycobacterial lipoarabinomannan induction of nitric oxide. *Infect Immun*. 2003;71(3):1442–1452.

21. Bauskin AR, et al. Role of macrophage inhibitory cytokine-1 in tumorigenesis and diagnosis of cancer. *Cancer Res*. 2006;66(10):4983–4986.

22. Li C, et al. GDF15 promotes EMT and metastasis in colorectal cancer. *Oncotarget*. 2016;7(1):860–872.

23. Zhang Z, et al. Opposing effects of PI3K/Akt and Smad-dependent signaling pathways in NAG-1-induced glioblastoma cell apoptosis. *PLoS ONE*. 2014;9(4):e96283.

24. Shi Y, Massagué J. Mechanisms of TGF-beta signaling from cell membrane to the nucleus. *Cell*. 2003;113(6):685–700.

25. Freudlsperger C, et al. TGF-β and NF-κB signal pathway cross-talk is mediated through TAK1 and SMAD7 in a subset of head and neck cancers. *Oncogene*. 2013;32(12):1549–1559.

26. Baldwin AS. Control of oncogenesis and cancer therapy resistance by the transcription factor NF-kappaB. *J Clin Invest*. 2001;107(3):241–246.

27. Schwitalla S, et al. Intestinal tumorigenesis initiated by dedifferentiation and acquisition of stem-cell-like properties. *Cell*. 2013;152(1-2):25–38.

28. Koliaraki V, Pasparakis M, Kollias G. IKKβ in intestinal mesenchymal cells promotes initiation of colitis-associated cancer. *J Exp Med*. 2015;212(13):2235–2251.

29. Wang J, et al. RelA/p65 functions to maintain cellular senescence by regulating genomic stability and DNA repair. *EMBO Rep*. 2009;10(11):1272–1278.

30. Lesina M, et al. RelA regulates CXCL1/CXCR2-dependent oncogene-induced senescence in murine Kras-driven pancreatic carcinogenesis. *J Clin Invest*. 2016;126(8):2919–2932.

31. Ruffell B, Coussens LM. Macrophages and therapeutic resistance in cancer. *Cancer Cell*. 2015;27(4):462–472.

32. Carbone C, Melisi D. NF-κB as a target for pancreatic cancer therapy. *Expert Opin Ther Targets*. 2012;16 Suppl 2:S1–10.

33. Döppler H, Liou GY, Storz P. Downregulation of TRAF2 mediates NIK-induced pancreatic cancer cell proliferation and tumorigenicity. *PLoS ONE*.

2013;8(1):e53676.

34. Wilson W, Baldwin AS. Maintenance of constitutive IkappaB kinase activity by glycogen synthase kinase-3alpha/beta in pancreatic cancer. *Cancer Res*. 2008;68(19):8156–8163.

35. Hu H, Jiao F, Han T, Wang LW. Functional significance of macrophages in pancreatic cancer biology. *Tumour Biol*. 2015;36(12):9119–9126.

36. Habtezion A, Edderkaoui M, Pandol SJ. Macrophages and pancreatic ductal adenocarcinoma. *Cancer Lett*. 2016;381(1):211–216.

37. Vaňhara P, Hampl A, Kozubík A, Souček K. Growth/differentiation factor-15: prostate cancer suppressor or promoter? *Prostate Cancer Prostatic Dis*. 2012;15(4):320–328.

38. Jiang YJ, et al. Establishment of an orthotopic pancreatic cancer mouse model: cells suspended and injected in Matrigel. *World J Gastroenterol*. 2014;20(28):9476–9485.

39. Yoshimura H, Matsuda Y, Naito Z, Ishiwata T. In Vivo Bioluminescence Imaging of Pancreatic Cancer Xenografts in NOG Mice. *J Carcinogene Mutagene*. 2013;S9:003.